Liquid Spray Impact onto Flat and Rigid Walls: Formation and Spreading of Accumulated Wall Film

Davood Kalantari[1] and Cameron Tropea[2]

Abstract: This study presents a combined experimental and theoretical investigation on the formation and spreading of a liquid film on a flat and rigid wall due to spray impact. A dual-mode phase Doppler instrument is used to characterise the spray while the average film thickness is measured using a high-speed CCD camera. The experimental results are complemented with theoretical expressions derived under the assumption that the spray is stationary. A new model for the prediction of the average wall film thickness is formulated taking into account the mean Reynolds number of the impacting drops, the flux density of the impacting droplets, and the average drop diameter. The theoretically determined average film thickness exhibits a good agreement with the measured data when the film can be considered thin.

Keywords: spray; spray impact; wall film; film thickness; Phase Doppler.

Nomenclature

A_d	Area of the impacting drop
A_{wall}	Area of the wall cell
C	Constant coefficient
P_{dyn}	Dynamic pressure of the impacting drop
u_b	Velocity normal to the wall before impact
u_a	Velocity normal to the wall after impact
v_b	Velocity parallel to the wall before impact
v_a	Velocity parallel to the wall after impact
Ω	Volume of boundary layer of the spreading droplet
We_{nb}	Weber number before impact_normal component

[1] Dep. of Mechanics of Biosystems Engineering, University of Sari (SANRU), P.O.Box 578, Sari, Iran. Email: dkalantari2000@yahoo.com

[2] Institute of Fluid Mechanics and Aerodynamics, Center of Smart Interfaces, Technische Universität Darmstadt, Darmstadt, Germany.

We$_{tb}$ Weber number before impact_tangential component
Oh   Ohnesorge number $\sqrt{We/Re}$
We   Weber number
Re   Reynolds number
x   Spatial coordinate perpendicular to wall
t   time
q   Flux of impinging or ejecting droplets
K$_{Cr}$ Non- dimensional splashing threshold
d   Drop diameter
D   Target diameter
D_{spray} Spray diameter at the target height
ε   Surface roughness
θ   Trajectory angle, void fraction
μ   Dynamic viscosity
ρ   density
σ   Surface tension

character

A	-		Area, coefficient
a	-		Coefficient
C	-		Coefficient
d	m		Drop diameter
D	m		Target diameter
f	1/s		Frequency
F	N		Force acting on a drop or bubble
g	m/s^2		Acceleration of gravity
h	m		Film thickness
K	-		Non- dimensional splashing threshold
L	m		Length scale
m	kg		Mass
N	-		Number of droplets
Oh	$\sqrt{We/Re}$	-	Ohnesorge number
P	N/m^2		Pressure
q			Flux of impinging or ejecting droplets
Re	$\rho u d_b/\mu$	-	Reynolds number
t	s		Time
u	m/s		Velocity normal to the wall
v	m/s		Velocity parallel to the wall

We	$\rho u^2 d_b/\sigma$	-	Weber number
X		m	Spatial coordinate perpendicular to wall
Z		m	Spatial coordinate parallel to wall

Greek character

α	-	Coefficient
β	-	Non-dimensional maximum droplet spreading diameter
δ	m	Film thickness
ε	m	Surface roughness
θ	°	Trajectory angle
μ	Kg/ms	Dynamic viscosity
ξ	-	Maximum dimensionless diameter
ρ	Kg/m^3	Density
σ	N/m	Surface tension
τ	-	offset parameter for a splashing crown
Ω	m^3	Volume of boundary layer of the spreading droplet

Subscript

0	Before the impact, initial value
10	Mean diameter
30	Sauter mean diameter
a	After impact
adv	Advancing
b	Before impact
B	Crown base
C	Crown
D	Drag
dep	Deposition
$diss$	Dissipation
g	Gas phase
H	Crown height
l	Liquid phase
max	Maximum
MV	Measurement volume
n	Normal component
sp	Spreading
t	Tangential component

Symbol

*	Dimensionless
$^{-}$	Average, mean
$'$	Fluctuation of the mean value
Σ	Sum
Δ	Second order of gradient operator

1   Introduction

With regard to the process of spray/wall interaction, it has become evident in recent years that the liquid film formed on the wall plays an important role in determining the velocity and size of ejected droplets as well as the deposited mass fraction, see e.g., Bai et al. (2002), Cossali et al. (1999). Nevertheless, the formation of a wall film is often neglected in spray impact models, although the prediction of average film thickness and average velocity is very important for many industrial applications (especially for those involving spray cooling systems or for fuel injection sprays onto heated walls, since the wall film significantly affects the efficiency of heat transfer on the surface). In some applications, it is desirable to eliminate the deposited film on the wall as far as possible (e.g. in internal combustion engines), whereas in other cases a maximum deposition is required (e.g. in spray coating, spray painting or agricultural sprayers). On the other hand, the induced fluctuations in the liquid layer formed on the rigid walls may decrease the quality of coated or painted surfaces.

The average film thickness can also affect the properties of the secondary spray, splashing threshold, ejected mass and number of secondary droplets. Results obtained by Rioboo et al. (2003) indicate that in the case of a thin liquid film, the splashing threshold depends only on the impact Weber or non-dimensional splash parameter (K-number) which is independent of the dimensionless film thickness, see below for further details. Also it is shown by Cossali et al. (1997) that in the case of a single drop impact onto a stationary liquid film, the number of secondary droplets decreases as the depth of liquid layer is increased. For purposes of indicating the influence of the average liquid film thickness on the splash limiting criterion, several expressions have been introduced in the past, for example $K_{Cr} = 2100 + 5880 \cdot \bar{h}^*$ ($\bar{h}^* = \bar{h}/d_b$, where $\bar{h}$ is the average film thickness and d_b is the drop diameter before impact) by Cossali et al. (1997), or $K_{Cr} = 1304 + 5032\bar{h}^*$ for $0.1 < \bar{h}^* \leq 1$ by Kalantari and Tropea (2006b). In these criteria, splashing occurs if K is above the critical value, where $K = Oh \cdot Re^{1.25} > K_{Cr}$, and Oh is the

Ohnesorge number defined as $Oh = \sqrt{We}/Re$. ($We = \rho_L u_b^2 d_b/\sigma$, where ρ_L is the density of the liquid, u_b is the drop velocity upon impact and σ is the surface tension, $Re = \rho_L u_b d_b/\mu$ where μ is the dynamic viscosity of the liquid)

A classification of film thickness formed on the wall due to a single drop or spray impact is proposed by Kalantari and Tropea (2006b) and summarized in Table 1 based on the measurement data obtained by Wang and Chen (2002).

Table 1: Classification of film thickness formed on the wall due to spray impact based on experimental data from Wang and Chen, (2002).

Dimensionless film thickness ($\bar{h}^*$)	Wall film condition	Variation of K_{Cr}	K_{Cr} correlation (for 70% glyc./water droplets)
$\bar{h}^* \leq 0.1$	wetted wall	constant	$\approx 1770 - 1840$
$0.1 < \bar{h}^* \leq 1$	thin liquid film	increasing	$5032\bar{h}^* + 1304$
$1 < \bar{h}^* \leq 2$	shallow liquid film	decreasing	$\approx 6100\bar{h}^* - 0.54$
$\bar{h}^* > 2$	deep liquid layer	constant (asymptotic value)	≈ 4050

Furthermore, it appears that the velocity fluctuations inside the accumulated wall film have a significant influence on the splashing phenomenon, since in a spray impact the crown base radius exhibits a growth rate proportional to $(t^* - \tau_R)^{nR}$; $0.2 \leq n_R \leq 0.32$, significantly different than that of a single droplet or train of single droplets impacting onto an undisturbed liquid layer, $\sim (t^* - \tau_R)^{0.5}$, as investigated theoretically by Yarin and Weiss (1995). ($t*$ is non-dimensional time $t^*=tu_b/d_b$ and τ_R is an offset parameter).

Numerous models exist regarding the formation of the wall film generated by an impacting liquid spray, see e.g., Stanton and Rutland (1996), Lee et al. (2001), and Bai and Gosman (1996), Ahmadi-Befuri et al. (1996), Kalantari and Tropea (2006e).

The model of Stanton and Rutland (1996) solves the continuity and momentum e-quations for a 2-D film flow over an arbitrary solid surface using the Euler method. This model considers many physical effects such as shear forces and dynamic pressure of impacting droplets, but neglects the Laplace (capillary) pressure arising from curvature of the air-liquid film interface. In this model the dynamic pressure

of impacting droplets is given as

$$P_{dyn} = \rho_L \sum_{i=1}^{N_b} \left(u_b^2 \left(A_d / A_{wall} \right) \right)_i \tag{1}$$

where u_b is the normal velocity component of the impacting droplet, A_d and A_{wall} are the area of the impacting droplet and wall cell area respectively.

The model of Lee et al (2001) propose another expression for the dynamic pressure of the impacting droplets

$$P_{dyn} = \left[(1 - \theta) \rho_L u_b^2 \right] \xi \tag{2}$$

where θ is the void fraction and ξ is a random number between zero and one; $\xi =$ rnd (0,1).

In the present study, experimental results are complemented by theoretical expressions regarding the hydrodynamics of liquid films under sprays, and preliminary models for the average wall film thickness are formulated.

2   Experimental methods and materials

The water spray was created using two different full-cone nozzles from Spraying System Co., operated at pressures between 3 and 7 bars. Two different, flat stainless steel targets with diameters of 5mm and 15mm (D=5 and 15mm) have been used in this study, using the end face of the cylinders, see Fig.1a. The entire target surfaces were covered by impacting spray in all experiments. The nozzles were placed at different positions above the target surface varying from 20 mm to 50 mm, e.g., x=-20. To characterise the spray, a dual-mode phase Doppler instrument from Dantec Dynamics was used, comprising a transmitting optics with a 400mm focal length, a receiving optics with a 310mm focal length, and an "A" type mask at a 34° scattering (off-axis) angle. The impacting and ejecting droplets were measured 1 mm above each target. The in-going and out-going droplets are distinguished using the sign of the velocity component normal to the target, i.e. positive u denotes an impacting droplet and a negative u denotes a secondary droplet, see Fig.1b.

Experimentally the wall film thickness has been characterised using a high-speed CCD camera. An example of this visualization and its evaluation are pictured in Fig. 2. The average film thickness was calculated by averaging many randomly chosen images obtained by the high-speed CCD camera.

For a flat and rigid target with diameter D under a symmetric spray, the general expression for computing the average film thickness across a diameter becomes $\bar{h} = \frac{1}{D} \int_{-D/2}^{D/2} h(r) dr$ (coordinate system given in Figure 1a).

$$We_{nb} = \rho_L \frac{u_b^2 d_b}{\sigma}$$

$$We_{tb} = \rho_L \frac{v_b^2 d_b}{\sigma}$$
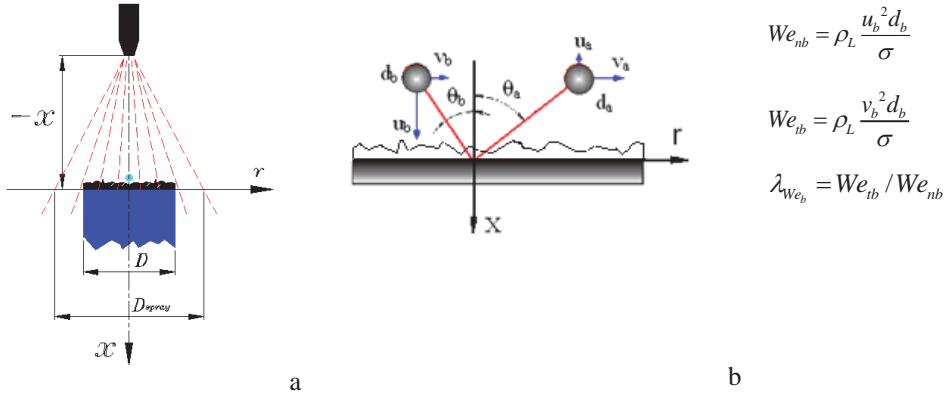
$$\lambda_{We_b} = We_{tb}/We_{nb}$$

Figure 1: a) Coordinate system and b) nomenclature for impinging and ejecting droplets.
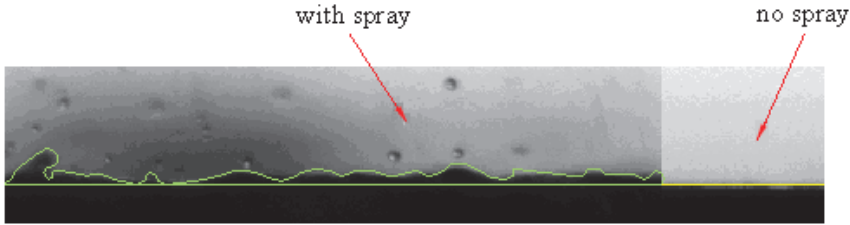

Figure 2: Thin liquid film formed under spray impact: original image of CCD camera with interface contour added.

In the present experiments the film thickness varied in the range $8\mu\text{m} \leq \bar{h} \leq 107\mu\text{m}$ and the standard deviation varied in the range ($5\mu\text{m} \leq \bar{\sigma}_h \leq 22.34\mu\text{m}$) for impingement Weber numbers in the range $10 < We_{nb} < 160$. (We_{nb} is the Weber number based on the normal component of the impact velocity u_b, defined by $We_{nb} = \rho_L u_b^2 d_b/\sigma$) and normal impact condition, i.e., $\lambda_{We_b} = We_{tb}/We_{nb} << 1$. ($We_{tb}$ is the Weber number based on the tangential component of the impact velocity v_b, defined by $We_{tb} = \rho_L v_b^2 d_b/\sigma$, see Fig. 1b. Note that these definitions are for a single droplet in a spray. For many droplets in spray, we compute the average of this quantity, e.g., $We_{nb} = \left(\sum_{i=1}^{N} \rho_{Li} u_{bi}^2 d_{bi}/\sigma\right)/N$. In the conducted experiments, this ratio falls in the range $\lambda_{We_b} \leq 0.023$, indicating that the tangential component of the impact velocity is negligible in this study.

An exemplary variation of the standard deviation of the film height fluctuations, σ_h, as a function of the measured average film thickness is illustrated in Fig. 3. It

is apparent from this data that the standard deviation of the measured film thickness does not correlate strongly with the measured average film thickness.
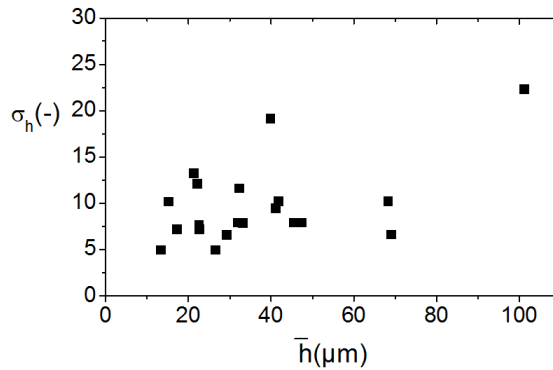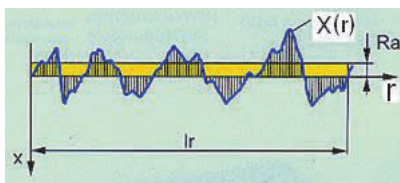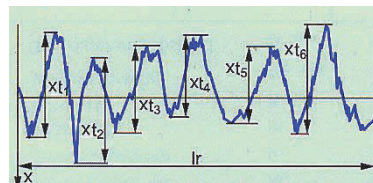

Figure 3: Example variation of the standard deviation σ_h as a function of the measured average film thickness.

The surface roughness of the rigid targets has been characterized by means of a mechanical profile meter from Hommelwerke Co., type TK300. Mean roughness (R_a or $\bar{\varepsilon}$) of the target surfaces used in this study ($R_a = \frac{1}{lr} \int_0^{lr} |x(r)| dr$, where lr is the measured length on the target surface) varied in the range 0.2 μm$<R_a <0.67\mu$m, whereas mean peak-to-valley roughness (R_Z) of the targets varied in the range 1.3 μm$<R_Z <6.6$ μm, see Fig.4. In this study, the relative surface roughness, either mean or peak-to-valley, in comparison to the mean measured drop size or average accumulated wall film thickness was negligible. More details of the measurement facilities and conditions used in collecting the experimental data can be found in Kalantari and Tropea (2007).

a   b

Figure 4: a) Mean roughness (R_a or $\bar{\varepsilon}$), and b) mean peak-to-valley roughness (RZ) of the target surface.)

3   Formation of the wall liquid film

In general, spray impingement on walls can be described by characterizing two aspects:

1. the generated secondary spray, and

2. the accumulated liquid wall film

The thickness of the accumulated wall film varies between microns to millimetres, depending on the condition of impacting spray and the boundary conditions on the target. Experimentally it is equally important to also capture the prevailing boundary conditions for any particular film, which in this case comprises the physical boundaries of the rigid surface (e.g. spherical target, flat plate, deep pool etc.,) and the characteristics of the impacting spray in terms of velocity, size and number density of impacting droplets.

Generally formation of the liquid film on a rigid-flat wall due to spray impact can be divided into the two different regions (Fig. 5);

1. The impingement region which is under influence of the impacting droplets and has a lower thickness, and

2. The outer region that is free of any impact phenomena. The film flow in this region depends on the film Reynolds number $Re_f = \rho \bar{u}_r \bar{h}/\mu$ and can be either laminar or turbulent.
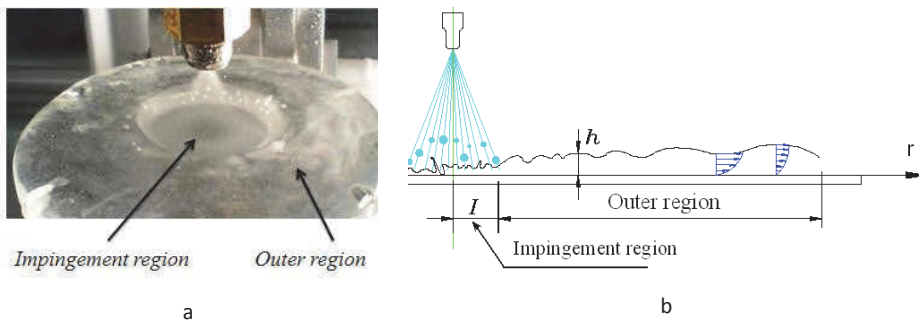

Figure 5: a) photograph of a spray impinging onto a large flat target, b) impingement and outer region of a liquid film formed under spray impact.

Practically measurement of the wall film thickness in the condition shown in Fig.5, where the target diameter is larger than the spray diameter is very difficult, since

the impingement region with lower film thickness is surrounded by the outer region, making observation of the impingement region impossible with high-speed camera; therefore we had to use targets with smaller diameter in compare to the spray diameter ($D_{spray} > D$) as illustrated in Fig.1a.

The measurement condition shown in Fig.1a has one more advantage: wall film flow in the impingement region is not influenced by the resistance of the film flow in the out region; therefore only the dynamic pressure created by the impinging droplets will be important for the liquid removal from the target surface.

Characterization of the accumulated wall liquid film under the spray impact can be achieved using:

- average film thickness ($\bar{h}$)

- average spreading film velocity ($\bar{u}_r$)

- velocity fluctuations inside the accumulated liquid film (u'_r)

In the impingement region of an inertial spray, the average film thickness created on the wall depends on the several parameters of the impacting spray ; normal and tangential component of impact velocity $\bar{u}_b$ and $\bar{v}_b$, volume flux density of impacting spray ($\dot{q} = q/A$; "q" and "A" to be volume flux of the impacting spray(m³/s) and the reference area over which flux is measured), volume-averaged diameter of impacting droplets (d_{30b}) defined by $d_{30b} = \left(\sum_{i=1}^{N} d_i^3 / N \right)^{1/3}$, density ($\rho_L\rho$) and dynamic viscosity of the liquid (μ), as well as the boundary condition of the target (e.g., flat or curved target surface or target surface completely covering with spray); average target surface roughness ($\bar{\varepsilon}^*$, where $\bar{\varepsilon}^* = \bar{\varepsilon}/d_{10b}$) and target size ($D$). A general expression for the average film thickness can be written as

$$\bar{h} = \psi \left(\bar{u}_b, \bar{v}_b, d_{30b}, \dot{q}, \rho_L, \mu, \bar{\varepsilon}^*, D_{spray}/D \right) \tag{3}$$

where, D_{spray} is the diameter of the effective impinging spray on the target defined as: $D_{spray} = 2x_{Nozzle} \cdot \tan(\alpha/2)$, α is the spray cone angle. The parameters $\bar{u}_b$, $\bar{v}_b$, d_{30b}, $\dot{q}$ and D_{spray} vary with nozzle pressure and nozzle height above the target. The three first parameters can be combined into an impact Reynolds or Weber number depending on the dimensional analysis output. Volume flux of impacting spray (q) depends on the atomizing pressure (P) with a power law; $q \propto P^{0.5}$ (Bernoulli's equation).

Two exemplary images of the thin liquid film formed on the rigid surface are presented in Fig. 6 for a relative sparse spray and for a relative dense spray. It is

apparent from these sample images (wavy form of the liquid film interface) that in describing the hydrodynamics of the film, e.g. velocity fluctuations inside the film, the capillary pressure will be non-negligible. Capillary pressure arising from the film interface curvature is described in section 3.1. Furthermore, the local film velocity will be an important parameter determining the outcome of any single drop impact event.
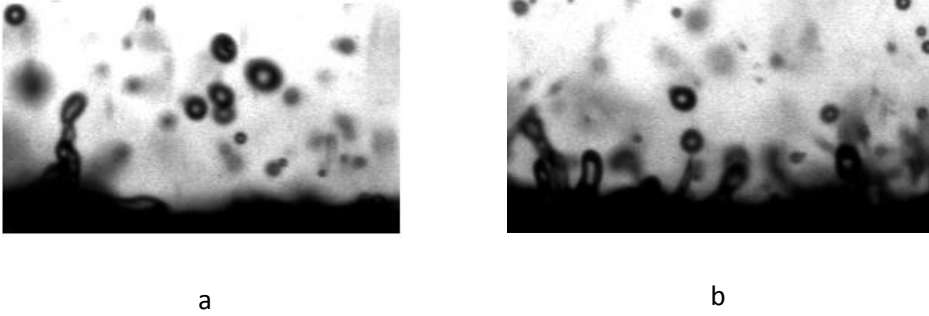

a   b

Figure 6: Sample images of the liquid film interface formed under spray impact: a) relatively sparse spray, b) relatively dense spray.

Assuming that the spray and the liquid film formed on the wall are isotropic in the $Y - Z$ plane, the conservation of mass equation for the control volume (CV) shown in Fig.7 yields

$$\sum \dot{m}_{in} - \sum \dot{m}_{out} = \frac{dm_{CV}}{dt} \tag{4}$$

In this equation $\dot{m}_{in}$ is the mass flux entering the control volume, i.e., mass flux of the impacting spray ($\dot{m}_b$), $\dot{m}_{out}$ is the mass flux leaving the control volume (mass flux of the secondary spray $\dot{m}_a$ in addition mass flux of the wall film leaving the control volume $\rho_l A_f \bar{u}_r$; where A_f is the area that the accumulated wall film leaves the target surface, defined by $A_f = 2\pi R \bar{h}$).

Since the spray and therefore the film flow are steady with time (i.e., dm_{CV}/dt=0); mass of the accumulated wall film and therefore the film thickness dose not change with time. In this case, conservation of mass equation (4) can be reduced to

$$\dot{m}_b - (\dot{m}_a + \rho_l A_f \bar{u}_r) = 0 \tag{5}$$

Rearranging this equation yields

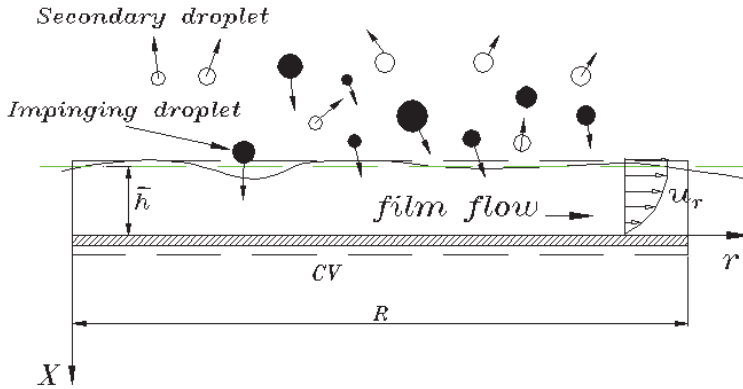$$\dot{m}_b - \dot{m}_a = \rho_l A_f \bar{u}_r \tag{6}$$

Figure 7: Control volume (CV) indicating impinging and ejecting droplet and wall film flow.

In the above equation, the value $\dot{m}_b - \dot{m}_a$ is the mass flux (m³/s) into the film from the spray (i.e., deposited mass flux into the film), and the right-hand-side indicates mass flux of the wall film leaving the target surface. In this equation the values $\bar{u}_r$ and $\dot{m}_b - \dot{m}_a$ must be estimated. The radial spreading velocity of the wall film ($\bar{u}_r$) can be obtained from the Navier-Stokes (momentum) equation, and mass source term of the wall film will be presented in section 3.2.

The momentum equation for radial direction in the cylindrical coordinate is

$$\rho \left(u_r \frac{\partial u_r}{\partial r} + \frac{u_\theta}{r} \frac{\partial u_r}{\partial \theta} - \frac{u_\theta^2}{r} + u_x \frac{\partial u_r}{\partial x} \right)$$
$$= -\frac{\partial P}{\partial r} + \mu \left[\frac{\partial}{\partial r} \left(\frac{1}{r} \frac{\partial (r u_r)}{\partial r} \right) + \frac{1}{r^2} \frac{\partial^2 u_r}{\partial \theta^2} - \frac{2}{r^2} \frac{\partial u_\theta}{\partial \theta} + \frac{\partial^2 u_r}{\partial x^2} \right] + \rho g_r \tag{7}$$

where u_r and u_θ are radial and peripheral spreading velocity of the wall film, respectively $\vec{u}_{film} = u_r \vec{e}_r + u_\theta \vec{e}_t$, see Fig. 8b.

In the following sections, different sources of the pressure term (P) will be discussed in detail.

3.1 Hydrodynamic pressure source in the wall liquid film

The source of the pressure term for the liquid film is

$$P = P_\sigma + P_0 + P_{dyn} \tag{8}$$

where P_σ is the Laplace pressure due to the curvature of the air-liquid film interface, P_0 is the pressure exerted by the ambient gas (air flow) onto the air-liquid interface
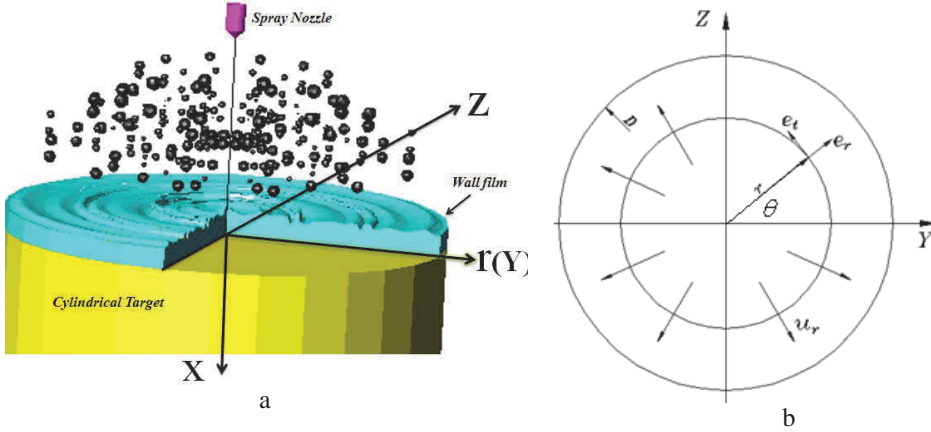
Figure 8: a) 3D-view of a liquid film on the target surface, b) top view of the target surface indicating radial spread of the accumulated film.

and P_{dyn} is the dynamic pressure exerted from impacting droplets, which is the main source responsible for spreading out and thinning of the liquid wall film in the impingement region.

On the other hand, the non-continuous nature of the impacting droplets causes the wavy form of the spreading liquid film interface, therefore the capillary pressure gradient (P_σ) arises from film interface curvature either in the inner or in the first part of the outer zone, expressed by

$$P_\sigma = -\frac{\sigma}{(1 + (dh/dr)^2)^{3/2}} \frac{d^2h}{dr^2} \qquad (9)$$

To a first approximation, we neglect the nonlinear terms involving the slope of the liquid-air interface ($dh/dr \ll 1$) to have a simpler and linear set of conditions at the interface, yielding

$$P_\sigma \cong -\sigma \frac{d^2h}{dr^2} \qquad (10)$$

In the outer region (Fig. 5), the Laplace pressure induced by the curvature of the air-liquid film interface is significantly smaller and fluctuations are negligible, since the surface is no longer wavy. With such assumptions the velocity profile across the film in the outer region can be considered in a quasi-steady-state form.

The main factor responsible for the spreading and thinning of the liquid film in the impingement region is the dynamic impingement pressure generated by the

impacting droplets. Introduction of the dynamic pressure arising from impacting droplets on a rigid wall is already given by Stanton and Rutland (1996) and Stanton and Rutland (1998). The normal component of the dynamic force exerted on the wall by an impacting drop is given by

$$F_{dyn} = (m_b u_b - m_a u_a) / \Delta t \qquad (11)$$

where subscripts a and b refer to after and before impact, respectively.

Defining the volume flow rate of the impacting drop by $q = \Delta V / \Delta t$, Eq. (11) can be rewritten as

$$F_{dyn} = \rho_L (q_b u_b - q_a u_a) \qquad (12)$$

Considering the definition of dynamic pressure ($P_{dyn} = F_{dyn}/A$) and flux density of impacting droplets $\dot{q}\,[m/s] = q/A$, (12) yields

$$P_{dyn} = \rho_L (\dot{q}_b u_b - \dot{q}_a u_a) = \rho_L \dot{q}_b u_b \left(1 - \frac{m_a u_a}{m_b u_b} \right) \qquad (13)$$

The coefficient $\beta = 1 - m_a u_a / (m_b u_b)$ in Eq. (13) takes into account the generated secondary droplets by an inertial impacting spray. By considering that u_a and u_b have different signs, a useful form of the coefficient β can be expressed in the form of

$$\beta \approx \min \left\{ 2, 1 + \lambda_m |\bar{u}_a / \bar{u}_b| \right\} \qquad (14)$$

Another simple approach for estimating the dynamic pressure of an impacting spray can be obtained by assuming that the rebounding drop has the same size and velocity as that of the primary drop, i.e. $d_a = d_b$ and $u_a = -u_b$; then the dynamic pressure exerted on the wall by a rebounding drop is

$$P_{dyn-reb} = 2\rho_L \dot{q}_b u_b \qquad (15)$$

The same procedure for a deposited droplet yields

$$P_{dyn-dep} = \rho_L \dot{q}_b u_b \qquad (16)$$

Some droplets rebound, some deposit, and some splash, therefore a constant factor β depending on the number of rebounding or depositing droplets can be considered for the hydrodynamic pressure exerted on the wall as

$$P_{dyn} = \beta \rho_L \dot{q}_b \bar{u}_b; \quad 1 < \beta < 2 \qquad (17)$$

For a spray, the coefficient β can be estimated based on the number of ejected droplets from the wall in comparison to all the primary droplets, defined as

$$\beta \approx \min\left\{2, \left(1 + \dot{N}_a/\dot{N}_b\right)\right\} \tag{18}$$

As an asymptotic condition, if all of the impacting droplets rebound from the wall or deposit on the wall, then the expression (18) gives $\beta = 2$ or $\beta = 1$, respectively. A value between 1 and 2 accounts implicitly also for those droplets which result in partial deposition. In the case of a normal impact condition ($\lambda_{We_b} < 0.1$), the ratio $\dot{N}_a/\dot{N}_b$ is estimated as (Kalantari and Tropea, 2007) , see Fig. 9.

$$\lambda_N = \left(\dot{N}_a/\dot{N}_b\right) = 2.16 \times 10^{-3} We_{nb} + 8.96 \times 10^{-2} \tag{19}$$
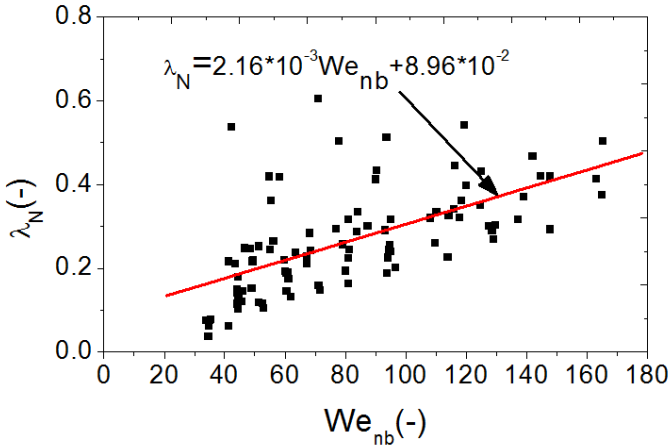

Figure 9: Total secondary-to-incident number ratio as a function of impact Weber number based on the normal velocity component.

Note that the ratio $\dot{N}_a/\dot{N}_b$ and N_a/N_b are identical in the spray/wall interaction, since the acquisition time for measuring the impinging and ejecting droplets from the wall is the same, i.e., $\lambda_N = \frac{\dot{N}_a}{\dot{N}_b} = \frac{N_a/\Delta T_a}{N_b/\Delta T_b} = \frac{N_a}{N_b} = \sum_{i=1}^{N_a} N_i \Big/ \sum_{j=1}^{N_b} N_j$; since $\Delta T_a = \Delta T_b$.

3.2 Mass source term of the wall liquid film

Mass source term of the wall liquid film in the conservation of mass equation (6) can be expressed as

$$\dot{m}_f = \dot{m}_b - \dot{m}_a = \left(1 - \dot{m}_a/\dot{m}_b\right)\dot{m}_b = (1 - \lambda_m)\dot{m}_b = (1 - \lambda_m)\rho_l A_{sp}\dot{q}_b \tag{20}$$

where λ_m is the secondary-to-incident mass ratio and A_{sp} is the cross section of the spray covering the target surface. In the case of a target surface exposing completely under the spray; $A_{sp} = \pi R^2$.

Results obtained by Kalantari and Tropea (2007) indicate that in the case of a normal spray impact, i.e., negligible tangential energy of impacting drops ($\lambda_{We_b} < 0.1$), the secondary-to-incident mass ratio (λ_m) lies in the range [0.002, 0.85], whereas this ratio moves to the range [0.016, 1.12] for oblique impact conditions ($\lambda_m \geq 0.1$). The results also indicate that in the case of a normal impact condition ($\lambda_{We_b} < 0.1$), the secondary-to-incident mass and number ratio, λ_m and λ_N, increase linearly with the impact Weber number based on the normal component of the impact velocity (We_{nb}).

$$\lambda_m = (\dot{m}_a/\dot{m}_b) = 6.74 \times 10^{-3} We_{nb} - 0.204 \tag{21}$$

The correlations (19) and (21) were derived from numerous measurements conducted in the range $35 \leq We_{nb} \leq 165$ and $\lambda_{We_p} < 0.08$, as illustrated in Fig. 9 and Fig. 10.
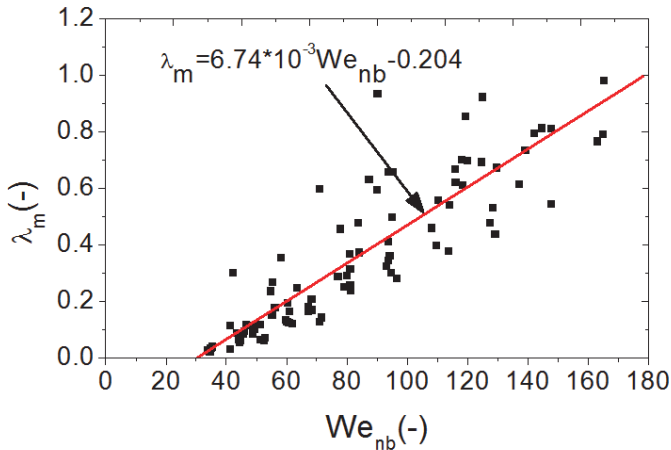

Figure 10: Total secondary-to-incident mass ratio as a function of impact Weber number based on the normal velocity component.

4   Approximate solution for the wall film thickness

Here an approximate solution (where the spray and spreading wall film are steady, $\partial/\partial t = 0$) for the wall film thickness is presented, valid for the assumptions given in section 2.

In the impingement region of a sparse, symmetric and stationary spray, we may assume that the frequency of the impacting drops is low enough, that the velocity fluctuations inside the film and also the air-liquid film interface fluctuations are damped ($\lambda >> \bar{h}$ or $\delta h << \bar{h}$, see Fig.11a) between the impact of two neighbor droplets. Under these conditions, the Laplace pressure arising from air-liquid film interface can be neglected. We may assume that the accumulated wall film only radially spread out (i.e., $u_\theta = 0$) and therefore the mean velocity inside the liquid film has only a radial component ($\bar{u}_r$), computed by

$$\bar{u}_r = \frac{1}{\forall_f} \int_0^{-\bar{h}} \int_0^{2\pi} \int_0^R u_r(r,\theta,x) r \, dr \, d\theta \, dx \tag{22}$$

which $\forall_f$ is the volume of fluid in the control volume, i.e., volume of the spreading film on the target surface under the stationary impacting spray.

The velocity profile inside the film $u_r(r,\theta,z)$ can be obtained from the momentum equation (7). considering the assumptions mentioned above, the momentum equation can be simplified into ($u_\theta = 0$ and $g_r=0$)

$$-\frac{\partial P}{\partial r} + \mu \left(\frac{\partial^2 u_r}{\partial x^2} \right) = 0 \tag{23}$$

One possible solution for this differential equation (23) can be derived by considering that the first term in (23) is constant in integrating over the x-component. After inserting the boundary condition ($x = 0, u_r = 0$) and ($x = -h \cong -\bar{h}, \tau_{yz} = \mu \frac{\partial u_r}{\partial x} = 0$), the following expression for the radial spreading velocity of the wall film can be obtained.

$$u_r = \frac{1}{\mu} \frac{\partial P}{\partial r} \left(x^2/2 + \bar{h}x \right) \tag{24}$$

where $u_r = \bar{u}_r + u'_r$

Substituting the obtained value for the radial velocity of the spreading film (24) into (22), and changing the integral limits, one achieves

$$\bar{u}_r = \frac{1}{(\pi R^2 \bar{h})} \int_0^{2\pi} \int_0^R \int_0^{-\bar{h}} \frac{1}{\mu} (\frac{\partial p}{\partial r}) r(x^2/2 + \bar{h}x) dx dr d\theta \tag{25}$$

However this expression is again difficult to solve for estimating the average radial spreading velocity of the accumulated wall film, because the values of $\partial P/\partial r$ must first be estimated. Neglecting the pressure term associated with the ambient gas flow and from the Laplace pressure, and assuming that dP associated by impacting
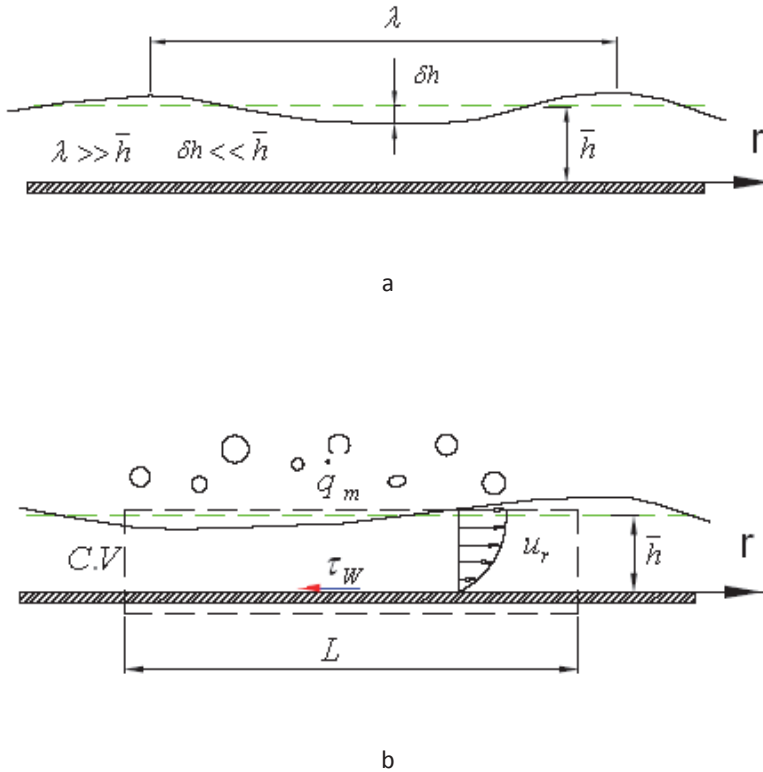
Figure 11: a) Curvature of the liquid film-air interface, and b) Control volume (CV) for a spreading wall liquid film.

droplet vanishes linearly in the radial direction; a simple form of $\partial P/\partial r$ can be considered as, see Fig.12.

$$\frac{dP}{dr} = \frac{P_2 - P_1}{r_2 - r_1} = \frac{C_1' P_1 - P_1}{C_1'' R} = -\frac{(1 - C_1') P_1}{C_1''} \frac{P_1}{R} = -C_1 P_{dyn}/R \tag{26}$$

Note that the value p_1 in (26) is dynamic pressure exerted from the impacting drop p_{dyn} (see Fig.12). Substituting (26) in (25) and integrating yields

$$\bar{u}_r = -\frac{C_1 \bar{h}^2 p_{dyn}}{3\mu R} \tag{27}$$

Combining the conservation of mass equation (6) with mass source term of the wall film (20), we obtain

$$(1 - \lambda_m)\rho_l A_{sp}\dot{q}_b = \rho_l A_f \bar{u}_r \tag{28}$$
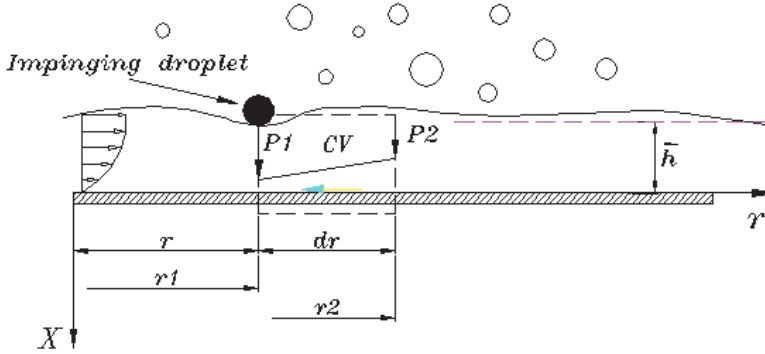
Figure 12: Variation of the dynamic pressure due to the impinging droplets in a spray.

Substituting the average spreading velocity of the wall film (27) into (28) yields

$$\bar{h} = - \left[\frac{3\mu(1-\lambda_m)\dot{q}_b R^2}{2C_1 P_{dyn}} \right]^{1/3} \tag{29}$$

Note that the minus sign of the film thickness is due to the vertical coordinate choosed downward. Considering again the dynamic pressure of the impacting spray (17) and substituting into (29), one obtains after simplifications and non-dimensionalizing the average film thickness by average impacting droplet diameter (d_{10b}).

$$\bar{h}/d_{10b} = CRe_b^{-1/3} \left[3\beta^{-1}(1-\lambda_m)d_{10b}^{-2}D^2 \right]^{1/3} \tag{30}$$

In this expression, $C(C = - (2C_1)^{-1/3})$ is a constant coefficient. The coefficient C depends on the surface roughness, wall temperature and maybe the surface material, and is found to be equal to 32 for the measurements reported in this study based on the target diameter (D) in *mm* and d_{10b} in *micron*. The Re_b given in (30) is average Reynolds number of impacting droplets. At a given measurement point, this value can be computed by $Re_b = \left(\sum_{i=1}^{N} \rho_{Li} u_{bi} d_{bi}/\mu \right)/N$ for a normal impact condition.

5   Results and discussion

Two exemplary results of the average film thickness ($\bar{h}$) together with the impact Weber number (We_{nb}), mass ratio (λ_m) and flux density ($\dot{q}$) are illustrated in Figs. 13a and 13b as a function of nozzle height (x) for two different nozzle pressures (3

and 6 bar) for a stainless steel target with diameter of 5mm ($D = 5mm$). It should be noted that both impact Weber number and flux density of impacting drops decrease with the nozzle height. It is shown in this figure that decreasing the impact Weber number yields an increase in the accumulated wall film thickness but a decrease of the secondary-to-incident mass ratio (λ_m). The same behaviour was observed for the secondary-to-incident number ratio (λ_N). Note that in the experiments, the entire target surface was exposed to the impacting spray, i.e., $D_{spray}/D > 1$.
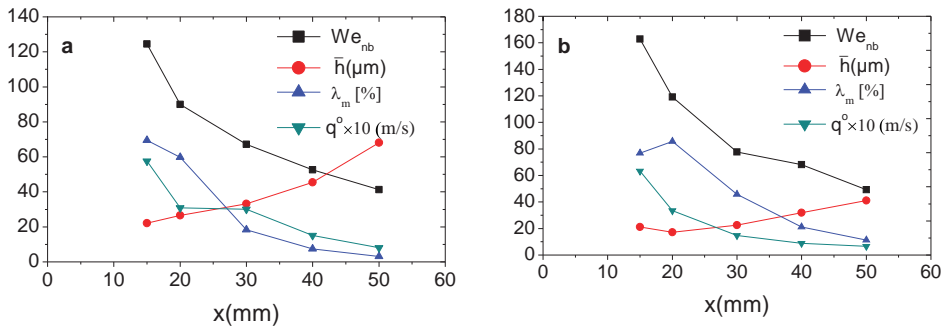

Figure 13: Variation of the impact Weber number (We_{nb}), average film thickness ($\bar{h}$), mass ratio(λ_m) and flux density ($\dot{q}$) with the nozzle height (x) for two exemplary nozzle pressures: (a) 3 bar, and (b) 6 bar; for a stainless steel target with diameter of 5mm ($D = 5mm$).

The dimensionless average film thickness accumulated on the flat-rigid wall as a function of Reynolds number before the impact is presented in Fig.14 together with the predictions obtained from Eq. 30. Results in this figure indicate that the dimensionless average film thickness decreases significantly with the impact Reynolds number. Results presented in this figure also indicate that the theoretical prediction presented in this study (Eq. 30) yields good agreement with the experimental data, mostly for the thin or shallow liquid film conditions, Kalantari and Tropea (2007).

In the experiments presented in this figure (Fig. 14), the normal velocity component varies in the range $8 \ m/s \leq \bar{u}_b \leq 18 \ m/s$, the flux density of the impacting spray varies in the range $0.5 \ m/s \leq \dot{q}_b \leq 16 \ m/s$, and the volume averaged droplet size varies in the range $53 \ \mu m \leq d_{30b} \leq 75 \ \mu m$.

The theoretical expression obtained for estimating the average film thickness on the wall (30) has been derived based on the laminar boundary-layer type film flow, i.e. $Re_{film} < 500$, and also examined for the lower mean Reynolds numbers in this study ($Re_{nb} < 700$). Therefore validity of this expression remains consistent for $Re_{film} < 500$. The dependency of the film thickness on the impact Reynolds
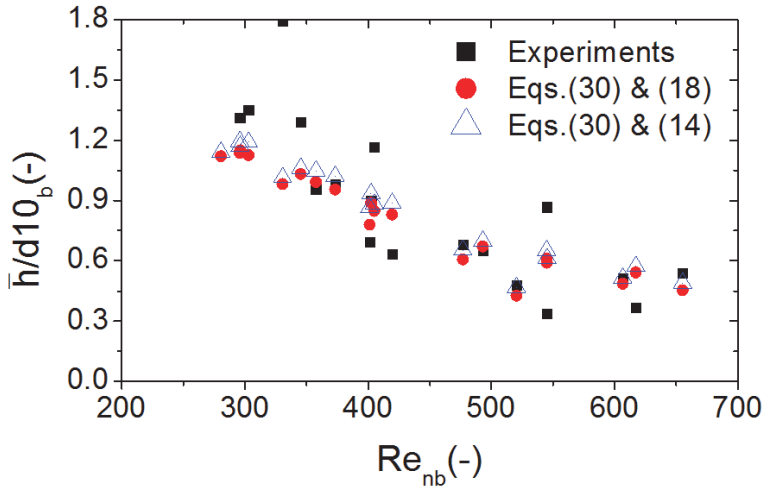
Figure 14: Average dimensionless film thickness accumulated on the flat-rigid wall as a function of Reynolds number before the impact.
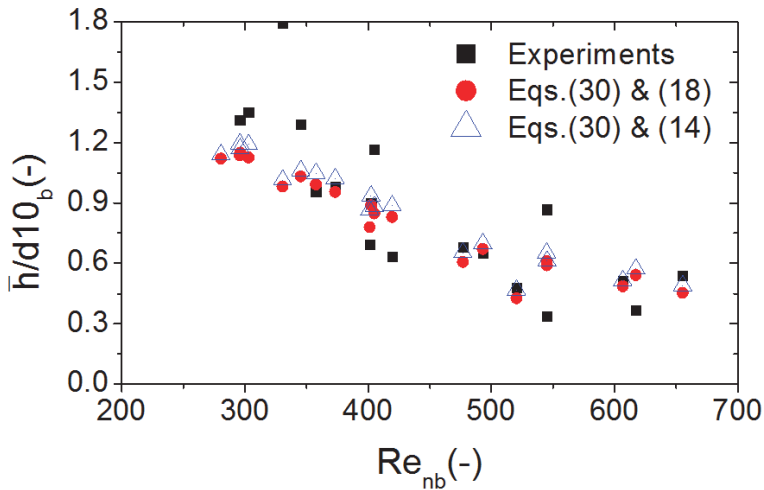

Figure 15: Variation of the non-dimensional thickness of the spreading lamella as a function of impact Reynolds number at the instant of d_0/u_0

number in this expression, i.e., $\bar{h}/d10_b \sim Re^{-1/3}$, is consistent with the results of Roisman et al. (2006) which is valid for low impact Reynolds numbers (Re<1000), see Fig.15.

The only important condition in estimation of the film thickness is that the entire

target surface should be exposed to the impacting spray ($D_{spray}/D > 1$).

6   Conclusions

This paper presents a new theoretical model for predicting the average film thickness as a function of mean Reynolds number of the impacting drops, flux density of the impacting droplets, and the average drop diameter. The theoretical derivation for the average film thickness exhibits good agreement with the measured data in the thin film condition, i.e. $\bar{h}^* = \bar{h}/d_{10b} \leq 1$. Results obtained in this study indicate a significant influence of the Reynolds number on the average film thickness accumulated on the wall due to liquid spray impact.

As illustrated above, the mean film thickness varied in the range $8\mu\mathrm{m} < \bar{h} < 107\mu\mathrm{m}$, corresponding to an impingement Weber number in the range $10 < \mathrm{We}_{nb} < 165$, based on the normal velocity component. In the case of constant impact Weber numbers, the average film thickness has a complex and non-predictable influence on the total secondary-to-incident mass ratio for the conducted measurements in this study, despite the fact that the dimensionless average film thickness falls in the thin liquid film condition $\bar{h}^* \leq 1$.

References

Ahmadi-Befrui, B.; Uchil, N.; Gosman, A. D.; Issa, R. I. (1996): Modelling and simulation of thin liquid films formed by spray wall interaction. *Soc. Automot. Eng.*, no. 960627.

Bai, C.; Gosman, A. D. (1995): Development of methodology for spray impingement simulation. *Soc. Automot. Eng.*, no. 950283, pp. 69-87.

Bai, C.; Gosman, A. D. (1996): Mathematical modelling of wall films formed by impinging sprays. *Soc. Automot. Eng.*, no. 960626.

Bai, C.; Rusche, H.; Gosman, A. D. (2002): Modeling of gasoline spray impingement. *Atom. and Sprays,* vol. 12, pp. 1-27.

Bussmann, M.; Chandra, S.; Mostaghimi, J. (2000): Modelling the splash of a droplet impacting a solid surface. *Phys. Fluids,* vol. 12, pp. 3121-3132.

Coghe, A.; Brunello, G.; Cossali, G. E.; Marengo, M. (1999): Single drop splash on thin film: Measurements of crown characteristics. ILASS-Europe 99, Toulouse, July. 5-7th.

Cossali, G. E.; Brunello, G.; Coghe, A.; Marengo, M. (1999): Impact of a single

drop on a liquid film: experimental analysis and comparison with empirical models. Italian Congress of Thermofluid Dynamics UIT, Ferrara, 30 June-2 July.

Cossali, G. E.; Coghe, A.; Marengo, M. (1997): The impact of a single drop on a wetted surface. *Exp. Fluids*, vol. 22, pp. 463-472.

Cossali, G. E.; Marengo, M.; Coghe, A.; Zhdanov, S. (2004): The role of time in single drop splash on thin film. *Exp. Fluids,* vol. 36, pp. 888-900.

Cossali, G. E.; Marengo, M.; Santini, M. (2005): Single-drop empirical models for spray impact on solid walls: A review. *Atom. and Sprays,* vol. 15, pp. 699-736.

Fedorchenko, A. I.; Wang, A. B. (2004): On some common feature of drop impact on liquid surfaces. *Phys. of Fluids*, vol. 16, pp. 1349-1365.

Kalantari, D.; Tropea, C. (2007): Spray impact onto flat and rigid walls: Empirical characterization and modelling. *Int. J. Multiphase Flow,* vol. 33, pp. 525-544.

Kalantari, D.; Roisman, I. V.; Tropea, C. (2006): Spray impact onto deep liquid layers: deformation of air-liquid film interface, secondary spray and air bubble entrainment. ICLASS06, Aug.27-Sep.01, Kyoto, Japan.

Kalantari, D.; Tropea, C. (2005): Experimental study of spray impact onto rigid walls, 20th ILASS-Europe, Orleans, Sept. 5-7th.

Kalantari, D.; Tropea, C. (2006a): Phase-Doppler measurements of spray/wall interaction. *Exp. Fluids,* vol. 43, pp. 285-296.

Kalantari, D.; Tropea, C. (2006b): Comparison splash of a droplet in isolation and in a spray. Spray Workshop 2006, Mai. 29-30, Lampoldshausen, Germany.

Kalantari, D.; Tropea, C. (2006c): Oblique spray impingement onto rigid walls: Description of secondary spray. 14th Int. Mech. Eng. Conference, May.16-18, Isfahan, Iran.

Kalantari, D.; Tropea, C. (2006d): Spray impact onto rigid walls: Formation of the liquid film. ICLASS06, Aug.27-Sep.01, Kyoto, Japan.

Ko, K.; Arai, M. (2002): Diesel spray impinging on a flat wall, part I: Characteristics of adhered fuel film in an impingement diesel spray. *Atom. & Sprays,* vol. 12, pp. 737-751.

Lee, S. H.; Ko, G. H.; Ryou, H. S.; Hong, K. B. (2001): Development and application of a new spray impingement model considering film formation in a Diesel engine. *KSME International Journal,* vol. 15, pp. 951-961.

Manzello, S. L.; Yang, J. C. (2002): An experimental study of a water droplets impinging on a liquid surface. *Exp. Fluids,* vol. 32, pp. 580-589.

Moreira, A. L. N.; Moita, A. S.; Panao, M. R. (2010): Advances and challenges in explaning fuel spray impingement: How much of single droplet impact research

is useful?. Progress in Energy and Combustion Science.

Mundo, C.; Tropea, C.; Sommerfeld, M. (1997): Numerical and experimental investigation of spray characteristics in the vicinity of a rigid wall. *Exp. Therm. Fluid Sci.,* vol. 15, pp. 228-237.

Mundo, C.; Sommerfeld, M.; Tropea, C. (1995): Droplet-wall collisions: experimental studies of the deformation and breakup processes. *Int. J. Multiphase Flow,* vol. 21, pp. 151-173.

Mundo, C.; Sommerfeld, M.; Tropea, C. (1998): On the modeling of liquid sprays impinging on surfaces. *Atom. and Sprays*, vol. 8, pp. 625-652.

Naber, J. D.; Reitz, R. D. (1988): Modelling engine spray/wall impingement, SAE 880107.

Panão, M. R. O.; Moreira, A. L. N. (2005): Flow characteristics of spray impingement in PFI injection systems. *Exp. Fluids,* vol. 39, pp. 364-374.

Pasandideh-Fard, M.; Bhola, S.; Chandra, S.; Mostaghimi, J. (1998): Deposition of tin droplets on a steel plate: simulations and experiments. *Int. J. of Heat and Mass Transfer*, vol. 41, pp. 2929-2945.

Pasandideh-Fard, M.; Bussmann, M.; Chandra, S.; Mostaghimi, J. (2002): Simulating droplet impact on a substrate of arbitrary shape. *Atom. and Sprays,* vol. 11, pp. 397-414.

Pasandideh-Fard, M.; Chandra, S.; Mostaghimi, J. (2002): A three-dimensional model of droplet impact and solidification. *Int. J. of Heat and Mass Transfer,* vol. 45, pp. 2229-2242.

Pasandideh-Fard, M.; Mostaghimi, J. (1996): On the spreading and solidification of molten particles in a plasma spray process: effect of thermal contact resistance. *Plasma Chemistry and Plasma Processing,* vol. 16, pp. 83-98.

Pasandideh-Fard, M.; Qiao, M.; Chandra, Y. M.; Mostaghimi, M. (1996): Capillary effects during droplet impact on a solid surface. *Physics of Fluids*, vol. 8, pp. 650-659.

Range, K.; Feuillebois, F. (1998): Influence of surface roughness on liquid drop impact. *J. of Colloid and Interf. Science,* vol. 203, pp. 16-30.

Rioboo, R.; Bauthier, C.; Conti, J.; Voue, M.; De Coninck, J. (2003): Experimental investigation of splash and crown formation during single drop impact on wetted surfaces. *Exp. Fluids,* vol. 35, pp. 648-652.

Rioboo, R.; Marengo, M.; Tropea, C. (2001): Outcomes from a drop impact on solid surface. *Atom. and Sprays,* vol. 11, pp. 155-164.

Roisman, I. V.; Horvat, K.; Tropea, C. (2005): Spray impact: rim transverse

instability initiating fingering and splash, and description of a secondary spray. *Phys. of Fluids,* vol. 18, pp. 102104.

Scardovelli, R.; Zaleski, S. (1999): Direct numerical simulations of free surface and interfacial flow. *Ann. Rev. of Fluid Mechanics,* vol. 31, pp. 567-603.

Schmehl, R.; Rosskamp, H.; Willman, M.; Wittig, S. (1999): CFD Analysis of spray propagation and evaporation including wall film formation and spray/film. *Int. J. Heat and Fluid Flow,* vol. 20, pp. 520-529.

Senda, J.; Kobayashi, M.; Iwashita, S.; Fujimoto, H. (1994): Modelling of gasoline spray impingement on a flat wall. *Soc. Automot. Eng.*, no. 941894.

Sikalo, S.; Tropea, C.; Ganic, E. N. (2005): Impact of droplets onto inclined surfaces. *J. Colloid and Interface Science,* vol. 286, pp. 661-669.

Sivakumar, S.; Tropea, C. (2002): Splashing impact of a spray onto a liquid film. *Phys. Fluids Lett.*, vol. 14, pp. 85-88.

Stanton, D. V.; Rutland, C. J. (1998): Multi-dimensional modeling of thin liquid films and spray-wall interactions resulting from impinging sprays. *Int. J. Heat Mass. Trans*, vol. 41, pp.3037-3054.

Stanton, D. W.; Rutland, C. (1996): Modeling fuel film formation and wall interaction in Diesel engines. *SAE paper,* no. 960628.

Tropea, C.; Roisman, I. V. (2000): Modeling of spray impact on solid surfaces. *Atom. and Sprays,* vol. 10, pp. 387-408.

Tropea, C.; Marengo, M. (1998): The impact of drops on walls and films, ICMF 98, Lyon, France.

Wang, A.-B.; Chen, C.-C.; Hwang, W.-C. (2002): On some new aspects of s-plashing impact of drop-liquid surface interactions, in: Drop-surface interactions, edited by Rein, M., Springer Alert Pub.-Co.

Wang, M.; Watkins, A. P. (1993): Numerical modelling of Diesel spray impaction phenomena. *Int. J. Heat Fluid Flow,* vol. 14, pp. 301-311.

Yarin, A. L.; Weiss, D. A. (1995): Impact of drops on solid surfaces: self-similar capillary waves, and splashing as a new type of kinematics discontinuity. *J. Fluid Mech.*, vol. 238, pp. 141-173.